Science of the Total Environment 409 (2011) 5177–5187

Contents lists available at SciVerse ScienceDirect

Science of the Total Environment

journal homepage: www.elsevier.com/locate/scitotenv

Multiple effects and uncertainties of emission control policies in China: Implications for public health, soil acidification, and global temperature

Yu Zhao [a,b,*], Michael B. McElroy [a], Jia Xing [b], Lei Duan [b], Chris P. Nielsen [a], Yu Lei [a,c], Jiming Hao [b]

[a] School of Engineering and Applied Sciences, Harvard University, 29 Oxford St, Cambridge, MA 02138, USA
[b] School of Environment, Tsinghua University, Beijing 100084, China
[c] China Academy for Environmental Planning, Atmospheric Environment Institute, 8 Dayangfang BeiYuan Road, Chaoyang District, Beijing 100012, China

ARTICLE INFO

Article history:
Received 22 February 2011
Received in revised form 1 August 2011
Accepted 9 August 2011
Available online 22 September 2011

Keywords:
Emission control
Multiple effects
Uncertainty
China

ABSTRACT

Policies to control emissions of criteria pollutants in China may have conflicting impacts on public health, soil acidification, and climate. Two scenarios for 2020, a base case without anticipated control measures and a more realistic case including such controls, are evaluated to quantify the effects of the policies on emissions and resulting environmental outcomes. Large benefits to public health can be expected from the controls, attributed mainly to reduced emissions of primary PM and gaseous PM precursors, and thus lower ambient concentrations of $PM_{2.5}$. Approximately 4% of all-cause mortality in the country can be avoided (95% confidence interval: 1–7%), particularly in eastern and north-central China, regions with large population densities and high levels of $PM_{2.5}$. Surface ozone levels, however, are estimated to increase in parts of those regions, despite NO_X reductions. This implies VOC-limited conditions. Even with significant reduction of SO_2 and NO_X emissions, the controls will not significantly mitigate risks of soil acidification, judged by the exceedance levels of critical load (CL). This is due to the decrease in primary PM emissions, with the consequent reduction in deposition of alkaline base cations. Compared to 2005, even larger CL exceedances are found for both scenarios in 2020, implying that PM control may negate any recovery from soil acidification due to SO_2 reductions. Noting large uncertainties, current polices to control emissions of criteria pollutants in China will not reduce climate warming, since controlling SO_2 emissions also reduces reflective secondary aerosols. Black carbon emission is an important source of uncertainty concerning the effects of Chinese control policies on global temperature change. Given these conflicts, greater consideration should be paid to reconciling varied environmental objectives, and emission control strategies should target not only criteria pollutants but also species such as VOCs and CO_2.

1. Introduction

Driven by rapid socioeconomic development and intensive energy use, emissions of atmospheric pollutants and their impacts have evolved into a serious environmental challenge for China. National emissions of SO_2 were reported at a level of 23 Mt in 2008 (MEP, 2009), higher than total emissions in the same year of 17 Mt for Europe (CEIP, 2010) or 11 Mt for the U.S. (USEPA, 2010). Emissions of NO_X were reported at 16 Mt (MEP, 2009), close to results for the U.S. (USEPA, 2010). Due to these elevated emissions, a variety of environmental effects have been demonstrated. These include: high concentrations of primary and secondary particulate matter (PM), the pollutant of greatest concern for urban air quality (Lin et al., 2010), associated with serious effects on public health (WB and SEPA, 2007; Ho and Nielsen, 2007); elevated concentrations of ozone in some cities (T. Wang et al., 2006); and the highest levels of acidity for precipitation in the world, observed in parts of southern China (Wang and Xu, 2009).

Under environmental pressure, China's government is attempting to shift its development mode from one dependent on intense fossil energy inputs with consequent high emissions to a more resource-efficient and environment-friendly alternative. Compulsory and stringent emission control policies are being or will be implemented for relevant sources, targeting a range of atmospheric pollutants. These measures include: replacement of small, inefficient electric power generating units with larger and more efficient ones; installation of flue gas desulfurization (FGD) systems for all new thermal power units since 2005 (Zhao et al., 2008); installation of selective catalyst reduction (SCR) systems for thermal power units in “key areas” after 2010 (i.e., those with high densities of population and emissions, including north-central, south-central, and eastern China); improved regulation of emissions from cement production since 2005; and staged improvements in regulation of emissions from vehicles.

The environmental impacts of emission control on different species, however, can be complicated, resulting in conflicting outcomes. Conflicts include: (1) reduction of NO_X emissions may lead to higher

* Corresponding author at: School of Engineering and Applied Sciences, Harvard University, 29 Oxford St, Cambridge, MA 02138, USA. Tel.: +1 617 496 2410; fax: +1 617 384 8016.
E-mail address: yzhao@seas.harvard.edu (Y. Zhao).

0048-9697/$ – see front matter
doi:10.1016/j.scitotenv.2011.08.026

levels of O_3 in some regions, due to complex, nonlinear photochemistry (Lou et al., 2010; X. Tang et al., 2010; Zhou et al., 2010); (2) reduction of PM emissions can increase soil acidification by decreasing alkaline base cation deposition (Larssen and Carmichael, 2000; Zhao et al., 2007); and (3) reduction in emissions of reflective aerosols may increase the risk of global warming (Carmichael et al., 2002; Saikawa et al., 2009). Piecemeal focus on particular pollutants or end points, therefore, may fail to recognize side effects of emission control measures and may lead to misdirected policy decisions. Analysis of multiple effects is needed to evaluate the comprehensive benefits of possible emission abatement strategies in China.

Although the effects of Chinese air pollution and possible future scenarios have been studied previously (Carmichael et al., 2002; Saikawa et al., 2009), the environmental impacts of national emission control measures actually proposed by the government have not been assessed as yet using a comprehensive, multiple-effect framework. Moreover, uncertainties of these impacts have not been quantified statistically, limiting awareness of the risks of unintended adverse consequences. Accordingly, the current study conducts a thorough multiple-effect analysis to better understand the impacts of air pollution control policy in China. Two scenarios, a base case keeping current emission control levels, and a more realistic case including anticipated control measures in the future, are explored to evaluate the impact of associated emissions of atmospheric pollutants for a target year of 2020. Based on the differences in emissions implicated in the two scenarios, the effects of controls on public health, soil acidification, and global temperature are estimated based on a comprehensive understanding of the physics and chemistry of related species. Through probability assumptions for relevant parameters, uncertainties of those effects are quantified using Monte Carlo simulations.

2. Methods

2.1. Emissions

For the base year of 2005, Chinese emissions of SO_2, NO_X, total PM, PM_{10}, $PM_{2.5}$, black carbon (BC), organic carbon (OC), NH_3, and base cations (Ca^{2+} and Mg^{2+}) are estimated using a comprehensive bottom-up methodology as detailed in Zhao et al. (2011a), by which emissions are calculated as products of emission factors and activity levels by sector and region. Changes of emission factors and activity levels for the period 2005–2020 are summarized for the two scenarios in Table 1. Base and control scenarios are evaluated using the same activity levels but with different emission control levels assumed to apply in 2020. The activity levels are taken mainly from projections for future fossil energy use (IEA, 2007), industrial production (CAEP and SIC, 2009), and consumption of oil in the transportation sector (M. Wang et al., 2006). Specifically, CAEP and SIC (2009) projected the economy growth and industrial production by sector following the national polices of energy saving and emission reduction, and the results are believed to reflect the probable sectoral shift in the economy. The fast increase of oil consumption by on-road transportation and the decrease of solid fuel use (including coal and biofuel) for rural residential combustion reflect the urbanization process that is currently taking place in China.

In the base scenario, 2020 emission factors are taken as unchanged from 2005 national average levels in all industries except for the thermal power, transport, and cement sectors. In these industries, the sector average emission factors decrease not because of new emission control measures after 2005 but due to technology shift already mandated in 2005. By 2020, small and inefficient units will continuously be replaced with large and advanced ones, and FGD systems, low-NO_X burners (LNB), and electrostatic precipitators (ESP) will become more prevalent, reducing sector emission factors over time. Similarly, the increasing proportion of vehicles meeting stages II and III emission standards (equivalent to Euro II and III, respectively) are expected to decrease overall emission factors for the transport sector. Regarding cement production, changes in sector emission factors will result from the continued penetration of precalciner kilns and retirement of shaft kilns; emission factors for SO_2 are expected to decrease, but the benefits are likely to be offset by increases in emission factors for NO_X (Lei et al., 2011).

In the more realistic control scenario, emission factors for the key emitting sectors are assumed to be reduced further due to tightened control measures, elaborated as follows. Besides power plants, deployment of FGD is expanded to iron & steel production, and the SO_2 removal efficiency, currently estimated at 70%, is assumed to improve to 80%. We assume SCR systems are applied at power units in “key areas” as defined by the government. The control effects of SCR are only partial, and the average NO_X removal efficiency in 2020 is estimated at 40% and 50% for units built before and after 2010, respectively (Zhao et al., 2010). In transportation, stage IV and V standards are assumed to be required for on-road vehicles after 2010 and 2012, respectively. It is assumed that fabric filters (FF) will be widely applied in cement production, leading to a significant reduction in PM emission factors, and emission factors for SO_2 and NO_X will be further reduced due to improved removal efficiencies compared to the base case (Lei et al., 2011).

The ancillary benefits of emission control technologies across species are included in both scenarios, noting the larger effect that they have in the control scenario. For example, wet-FGD systems applied for SO_2 control in the power and iron & steel sectors lead also to reductions of PM. Also in both scenarios, no changes are assumed

Table 1
Changes of emission factors and activity levels for 2005–2020. All estimates are national averages for sectors. Indicated changes of activity levels concern production of brick and lime, and energy consumption in other sectors.

	Emission factor						Activity level
	Base			Control			
	SO_2	NO_x	PM	SO_2	NO_x	PM	
Power plant	−62%	−11%	−72%	−72%	−39%	−75%	110%
Cement	−23%	76%	0%	−50%	14%	−82%	60%
Iron & steel	0%	0%	0%	−80%	0%	−80%	117%
Other industry	0%	0%	0%	−15%	0%	−20%	40% Includes: −37% for brick making; −10% for lime production
On-road transport	−80%	−20%	−65%	−80%	−60%	−85%	161%
Non-road transport	−80%	−30%	−56%	−80%	−30%	−56%	27%
Residential (biofuel)	0%	0%	0%	0%	0%	0%	−20%
Residential (coal)	0%	0%	0%	−15%	0%	−20%	−5%
Biomass open burning	0%	0%	0%	0%	0%	0%	−20%

during 2005–2020 in NH_3 emission factors and in the mass fractions of PM that are BC, OC, and base cations, largely due to lack of effective technologies and targeting measures.

2.2. Chemical transport model

Concentrations of $PM_{2.5}$ and O_3, and depositions of sulfur and nitrogen are simulated using the Models-3/Community Multiscale Air Quality (CMAQ) system (V4.4). This model was previously applied to China in a number of regional and urban-scale air quality simulations (Streets et al., 2007; Wang et al., 2008; Fu et al., 2009) and has been validated using satellite and surface observations (Xing et al., submitted for publication). The modeling domain covers most of East Asia with a spatial revolution of 36×36 km. The driving meteorological inputs are provided by the fifth-generation NCAR/Penn State Mesoscale Model (MM5). Since this study focuses on annual estimates, one month representing each season (Jan, Apr, Jul, and Oct) was chosen and results were averaged subsequently. Monthly variations of emissions by sector are taken from Streets et al. (2003) and Zhang et al. (2007).

A policy-oriented, multi-layer Eulerian model is used to simulate long-range transport and deposition of base cations (Duan et al., 2007). The modeling domain covers the whole country with a grid resolution of 1°×1°. Precipitation data are obtained from the China Meteorological Administration, and wind fields from NCEP/NCAR reanalysis. The parameters of the model are calibrated by Hao et al. (2001), and the simulated total depositions of base cations are comparable to limited observations available for China (Duan et al., 2007; Zhao et al., 2011b).

2.3. Health effects and C–R functions

In this study, the health impacts of air pollution control are estimated on the basis of avoided premature mortality, and $PM_{2.5}$ and O_3 are the species of concern. The national avoided deaths due to reduced concentrations of these species can be calculated according to:

$$HE_i = \sum_j \Delta C_{i,j} \times \beta_i \times POP_j \times p_j \tag{1}$$

where i and j define the species and grid locations in the modeling domain, respectively; HE is the health effect (avoided premature deaths); ΔC is the reduced concentration from base to control scenario in 2020; β is the concentration–response (C–R) function; POP is the population; and p is the baseline annual mortality rate.

The population distribution is obtained through the China Census 2000 (CDC, 2003), with the total national population adjusted to 1.45 billion in 2020 according to the National Population Development Strategy Research (NPDSR, 2007). Possible changes in the spatial distributions of population, attributable for example to an expected increase in urbanization during the study period, are ignored in this study due to lack of data. The baseline annual mortality rates by province are taken from official statistics (NBS, 2006).

C–R functions are derived from integrated epidemiological evidence both for China and, when domestic information is lacking, for other parts of the world. With respect to acute mortality effects of PM, two studies for China using meta-analysis resulted in C–R functions of 0.30% (standard error: 0.10%) (Aunan and Pan, 2004) and 0.41% (95% confidence interval, CI: 0.25–0.56%) (HEI, 2004) increases, respectively, per 10 μg/m^3 increase in PM_{10} concentrations. A recent study of three cities in China (Wong et al., 2008) derived a similar C–R function of 0.37% (95% CI: 0.21–0.54%), and this result is applied here. Given the increasing attention to the health effects of $PM_{2.5}$ rather than PM_{10}, the C–R function is converted to 0.62% (95% CI: 0.35–0.90%) per 10 μg/m^3 increase in $PM_{2.5}$, with an assumed ratio of 0.6 for $PM_{2.5}$ relative to PM_{10} (Dockery and Pope, 1994). For the chronic mortality effects of PM, no cohort study has been conducted in China. Pope et al. (2002) found a C–R function of 4% (95% CI: 1–7%) per 10 μg/m^3 increase in $PM_{2.5}$ for the U.S. This result is adopted in the current study.

For the mortality effects of O_3, Levy et al. (2001) provided a pooled C–R function of 0.5% (95%: 0.3–0.7%) increase per 10 μg/m^3 increase of 24-h average O_3 from studies of U.S. cities. Wong et al. (2008) generated a similar value with a larger range (0.58%, 95% CI: 0.24–0.90%) for Chinese cities. We accepted this result here and converted it into a 1-h maximum concentration based value, i.e., 0.23% (95% CI: 0.10–0.36%), with an assumption that 1-h maximum concentrations are 2.5×24-h average ones (Levy et al., 2001).

2.4. Acidifying critical loads

Soil acidification is estimated by comparing the simulated deposition with critical load (CL), an indicator of ecosystem sensitivity. Based on given chemical criteria of ecosystems, CL defines the highest deposition level of an acidifying compound that will not cause chemical changes leading to long-term harmful effects on ecosystem structure and function (UBA, 2004). Although the CL concept simplifies the soil chemistry processes and thus brings some uncertainties, the concept has been widely applied in assessment of ecosystem acidification, dictating the required emission reduction of acidifying precursors, and in modeling the recovery process for threatened ecosystems in Europe (UBA, 2004; Hettelingh et al., 2007, 2008) and China (Hao et al., 2000; Zhao et al., 2009, 2011b). CL provides a reasonable basis for national-level policy making on emission control and acid rain mitigation.

Based on a steady-status mass balance (SSMB), CL can be expressed generally using Eqs. (2)–(4), by assuming that the sources of alkalinity must balance the input and production of acidity under steady-state conditions in the terrestrial ecosystem (UBA, 2004; Zhao et al., 2007). The critical molar ratio of base cations to aluminum (Al) in the soils is used as the chemical criterion indicating forest health:

$$S_D \le CL(S) = \begin{cases} BCs_D + CL(S)_{\text{limit}} & (N_D \le N_U + N_I) \\ BCs_D + CL(S)_{\text{limit}} - (1 - f_{DE}) \times (\mathrm{N_D} - \mathrm{N_U} - \mathrm{N_I}) & (\mathrm{N_D} > \mathrm{N_U} + \mathrm{N_I}) \end{cases} \tag{2}$$

$$CL(S)_{\text{limit}} = BCs_W - BCs_U - ANC_{L,crit} \tag{3}$$

$$ANC_{L,crit} = 1.5\frac{Bcs_D + Bcs_W - Bcs_U}{(Bcs/Al)_{crit}} + Q^{\frac{2}{3}}\left[1.5\frac{Bcs_D + Bcs_W - Bcs_U}{(Bcs/Al)_{crit} \cdot K_{gibb}}\right]^{\frac{1}{3}} \tag{4}$$

where S_D, N_D, and BCs_D are the depositions of sulfur, nitrogen, and base cations, respectively; BCs_W is the weathering rate of base cations from soil minerals; BCs_U and N_U are the vegetation uptake of base cations and nitrogen, respectively; N_I is the net immobilization rate of nitrogen in the soil; f_{DE} is the nitrate lost by denitrification; $ANC_{L,crit}$ is the critical leaching of alkalinity; Bcs_D, Bcs_W and Bcs_U are deposition, weathering rate, and vegetation uptake of base cations excluding Na (Na has no effect on buffering the toxicity of Al to vegetation; hence the notation *Bcs* is used as contrasted with *BCs* including Na); $(Bcs/Al)_{crit}$ is the critical molar ratio of base cations to Al in soils; Q is the precipitation surplus (precipitation minus evapotranspiration), water which percolates through the soil and then enters the surface water; and K_{gibb} is the dissolution constant for Al hydroxide.

The parameters for the CL calculation are mainly taken from Duan et al. (2002, 2004). CL maps across China were generated with a resolution of 36×36 km (the same as CMAQ), as described in detail by Zhao et al. (2009).

2.5. Global radiative forcing by emission precursor

In this study, the long-term global temperature response is estimated for Chinese emissions under the two scenarios, with the difference representing the effect of emission controls. The direct and indirect radiative forcing associated with each principal emission precursor (including SO_2, NO_X, BC, and OC) is applied in the evaluation, expressed as the emission-based constituent global forcing (CGF). The emission-based CGF represents that emissions of a single primary precursor can affect several forcing agents, e.g., emissions of NO_X affect the concentrations of methane (CH_4), tropospheric ozone, and tropospheric aerosols, all of which can impact radiative forcing. The effects of given species on radiative forcing and global temperature for a chosen time horizon, e.g., 100 years or 20 years, can be evaluated with integrated radiative forcing of the species, expressed as the energy added to the earth-atmospheric system during the time horizon due to the emissions. Since this work focuses only on the short-lived species which decay much faster than long-lived species such as CO_2 and do not cause additional forcing after the first 20 years, the integrated radiative forcing are essentially equal for the two time horizons for those aerosols and aerosol precursors (IPCC, 2007).

The global temperature change due to changes in emissions in China is calculated based on the CGF for each precursor, the fractional change due to Chinese emission changes, and the global climate sensitivity (Carmichael et al., 2002):

$$\Delta T = CS \times \sum_i \left(CGF_i \times \Delta E_{i,China} / E_{i,Global} \right) \quad (5)$$

where i stands for the species; ΔT is the global temperature change; CS is the climate sensitivity, taken as 0.75 K/W/m^2 (Carmichael et al., 2002); CGF is the emission-based constituent global forcing (W/m^2), taken from Carmichael et al. (2002) and IPCC (2007); $\Delta E_{i,China}$ is the change in emissions of species i in China during 2005–2020; and $E_{i,Global}$ is the global emission for species i.

The global emissions of SO_2, NOx, BC and OC in 2020 are obtained from the Current Legislation (CLE) scenario by Cofala et al. (2007). It should be noted that Cofala et al. (2007) did not include emissions from international shipping, aviation and biomass open burning, but indicated that SO_2 and NO_X emissions from those emitters are 13% and 44% from the sources covered in their estimate, respectively. These numbers are applied in this work to scale the global total emissions at 93 and 102 million metric tons (Mt) for SO_2 and NO_x, respectively, from anthropogenic sources. Regarding BC and OC, the emissions from biomass open burning are taken from Bond et al. (2004), and the global total emissions of BC and OC from anthropogenic sources are calculated at 8.1 and 34.0 Mt, respectively.

2.6. Uncertainty analysis

Monte Carlo simulation is used to quantify uncertainties in the impacts of the emission control measures. With probability distributions of parameters described below and summarized in Table 2, 1000 simulations were performed to generate the uncertainties and to identify parameters making most significant contributions to the uncertainties.

For the concentrations and depositions, the normalized mean error (NME), an indicator of the deviation between observed and simulated results, is applied here to approximate the uncertainties (Zhang et al., 2006). Since there are currently no published official concentrations for $PM_{2.5}$, daily averages of PM_{10} concentrations for all of the provincial capitals are used instead and the NME is calculated to be 42%, close to the result for $PM_{2.5}$ in the U.S (Zhang et al., 2009). The NMEs for O_3 are reported to as 20–22% for U.S (Zhang et al., 2009) and are tentatively adopted for this study, since they cannot be calculated more precisely given insufficient observations for O_3 in China. Based on limited observations of total deposition in

Table 2
The uncertainty assumptions for the parameters.

	Unit	Distribution	Range[a]	Correlation
$C_{PM2.5}$	μg/m^3	Normal	(−42%, 42%)	
C_{O3}	μg/m^3	Normal	(−22%, 22%)	
S_D	keq/ha/yr	Normal	(−34%, 34%)	BC_D 0.64; Bc_D 0.64; N_D 0.40
N_D	keq/ha/yr	Normal	(−50%, 50%)	BC_D 0.45; S_D 0.40
BCs_D	keq/ha/yr	Normal	(−60%, 60%)	Bc_D 0.76; S_D 0.64; N_D 0.45
Bcs_D	keq/ha/yr	Normal	(−60%, 60%)	BC_D 0.76; S_D 0.64
POP	Billion	Normal	(−10%, 10%)	
p	‰	Normal	(−20%, 20%)	
$\beta_{PM2.5}$ (acute)	%/(10 μg/m^3)	Normal	(−45%, 45%)	
$\beta_{PM2.5}$ (chronic)	%/(10 μg/m^3)	Normal	(−75%, 75%)	
β_{O3} (acute)	%/(10 μg/m^3)	Normal	(−55%, 55%)	
BCs_W; Bcs_W	keq/ha/yr	Uniform	(−60%, 60%)	
BCs_U	keq/ha/yr	Uniform	(−63%, 63%)	Bcs_U 0.90; N_U 0.75
Bcs_U	keq/ha/yr	Uniform	(−58%, 58%)	BCs_U 0.90
N_U	keq/ha/yr	Uniform	(−52%, 52%)	BCs_U 0.75
N_I	keq/ha/yr	Uniform	(−80%, 60%)	
f_{DE}	–	Uniform	(−20%, 20%)	
Q	m^3/ha/yr	Normal	(−40%, 40%)	
$(Bc/Al)_{crit}$	–	Uniform	(−50%, 50%)	
K_{gibb}	m^6/eq^2	Lognormal	(−62%, 166%)	
$E_{SO2,China}$	Mt	Lognormal	(−14%, 13%)	
$E_{NOx,China}$	Mt	Lognormal	(−13%, 37%)	
$E_{BC,China}$	Mt	Lognormal	(−25%, 136%)	
$E_{OC,China}$	Mt	Lognormal	(−40%, 121%)	
$E_{SO2,Global}$	Mt	Lognormal	(−14%, 16%)	
$E_{NOx,Global}$	Mt	Lognormal	(−27%, 37%)	
$E_{BC,Global}$	Mt	Lognormal	(−40%, 151%)	
$E_{OC,Global}$	Mt	Lognormal	(−47%, 120%)	
CS	K/(W/m^2)	Triangular	0.75 (0.50, 1.00)	
CGF_{SO2}	W/m^2	Triangular	−1.1 (−2.4, −0.5)	
CGF_{NOx}	W/m^2	Triangular	−0.22 (−0.44, 0)	
CGF_{BC}	W/m^2	Triangular	0.50 (0.15, 0.85)	
CGF_{OC}	W/m^2	Triangular	−0.20 (−0.40, 0)	

[a] The ranges are expressed as the 95% CIs around the mean values for parameters with normal and lognormal distributions, and as lower and upper limits around the mean values for those with uniform distributions. The ranges for CGF are expressed as the mean values with lower and upper limits.

China (Larssen et al., 2006), the NMEs for sulfur, nitrogen, and base cations are calculated as 34%, 50%, and 60%, respectively. The NMEs are used to determine the 95% CIs of the simulated results assuming normal distributions.

The 95% CIs for the C–R functions are described in Section 2.3. The 95% CIs for the total population and baseline mortality rate are taken to range ±10% and ±20% around the central estimate, respectively. Normal distributions are assumed for those parameters.

The estimates of BCs_W can vary significantly with different methods (Duan et al., 2002). In European studies the ranges of BCs_W are taken as ±33%–100% (Heywood et al., 2006) and BCs_W is estimated as a dominant parameter contributing to the uncertainty of CL (Skeffington et al., 2006, 2007). In this study, the ranges of BCs_W are estimated as ±60% from Duan et al. (2002), and we assume a uniform distribution. The ranges of vegetation uptakes of base cations and nitrogen are estimated as ±63% and ±52% from Duan et al. (2004), assuming uniform distributions. Since there is very little study on the $(Bcs/Al)_{crit}$ of Chinese vegetation, a uniform distribution with a typical European range (±50%) is tentatively applied here (Heywood et al., 2006). A lognormal distribution is assumed for K_{gibb}, as suggested by Li and McNulty (2007). Ranges for other parameters related to CL uncertainty are obtained from Zhao et al. (2007).

The uncertainties of emissions by species in China were estimated using Monte-Carlo simulations (Zhao et al., 2011a). The uncertainties of global SO_2 and NO_X emissions are currently unavailable. Those for Asia estimated by Streets et al. (2003), expressed as the relative changes of 95% CI around the central estimates, are adopted in this study to approximate the global uncertainties. The uncertainties of global BC and OC emissions are taken from Bond et al. (2004). Lognormal distributions are assumed for these emissions. The ranges of CGF are derived mainly from IPCC (2007), while the range of CS is taken as ±33% following the estimate by Carmichael et al. (2002). With the likeliest values and bounds, triangular distributions are applied to these parameters.

Besides the probability distributions, the correlations between certain parameters should be considered in the uncertainty analysis of CL and CL exceedance (Skeffington et al., 2007). Due to a lack of domestic analysis, European coefficients (Skeffington et al., 2007) for vegetation uptakes and depositions are used in this study, as summarized in Table 2.

3. Results and discussions

3.1. Emissions and simulated concentrations and depositions

The emissions in the base and control scenarios in 2020 are shown by sector in Fig. 1. Annual emissions in the base scenario are estimated as 30.7, 31.0, 37.7, 22.1, 14.7, 1.8, 3.0, 22.0, and 7.6 Mt of SO_2, NO_X, PM, PM_{10}, $PM_{2.5}$, BC, OC, NH_3, and base cations (Ca + Mg), respectively. Compared to 2005 (Zhao et al., 2011a), the emissions of NO_X and NH_3 increase most significantly among all species, by 57% and 29%, respectively. PM and base cations increase by 9% and 23%,

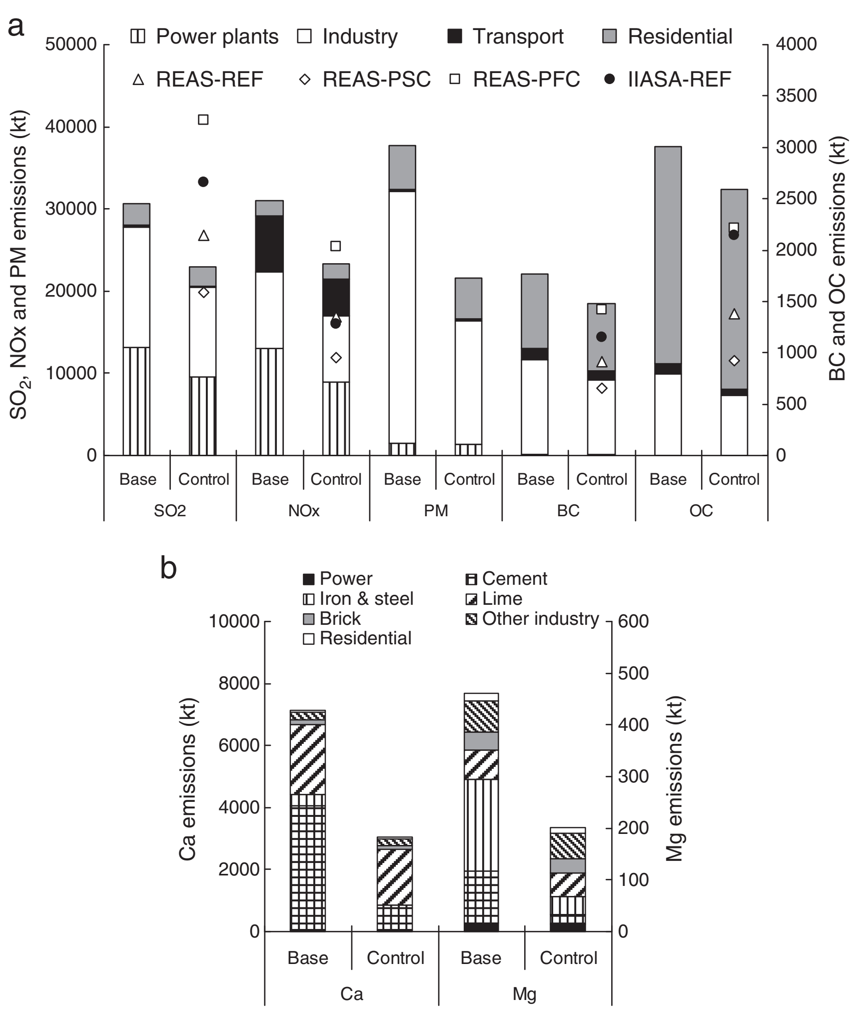

Fig. 1. Emissions in the base and control scenarios in 2020, compared with other studies. (a) SO_2, NO_X, PM, BC and OC; (b) Base cations: Ca and Mg. The abbreviations for scenarios by other studies include REF: Reference; PFC: Policy Failed Case; and PSC: Policy Succeed Case. Open biomass burning was not included in REAS scenarios.

respectively, while SO_2, BC, and OC emissions change slightly. Comparing base and control scenarios, PM and base cations are reduced most by the controls, by 43% and 57% respectively, due mainly to the wide application of FF in cement plants. The shares of total PM and Ca (the dominant base cation) from cement production decrease from 27% in the base scenario to 9% in the control scenario and from 56% to 24%, respectively. Both SO_2 and NO_X emissions are reduced by about 25%, due mainly to the improved removal efficiency of FGD and deployment of SCR systems, respectively. In particular, SO_2 and NO_X emissions from the power sector decrease by 27% and 32%, respectively. BC and OC emissions decrease less, by 16% and 14%, respectively, since no measures specifically targeting these two species are anticipated. Similarly lacking specific control measures, NH_3 emissions are assumed to be unchanged in the two scenarios.

Also indicated in Fig. 1 are the projected Chinese emissions for given species by other studies including REAS (Regional Emission Inventory in ASia) (Ohara et al., 2007) and estimates by IIASA (International Institution of Applied Systems Analysis) (Klimont et al., 2009). SO_2 emissions estimated here for the control scenario 2020 are generally lower than those included in other studies except for the REAS-PSC scenario. The difference reflects the fact that higher FGD penetration rates are assumed for the power and iron & steel sectors in this study. In contrast, NO_X emissions are generally higher than those in other studies, except the REAS-PFC scenario. Probable reasons for the difference include: (1) a conservative assumption in this study of the removal efficiency by SCR, based on the authors' field measurements (Zhao et al., 2010); and (2) inclusion in this study of rising emission factors from 2005 to 2020 in the cement sector. Since open biomass burning was not considered by REAS, BC and OC emissions in all of the REAS scenarios are lower than those in this study.

Fig. 2 indicates the differences of simulated annual-average concentrations of $PM_{2.5}$ and 1 h-max O_3, and also the depositions of sulfur, nitrogen, and base cations between the base and control scenarios in 2020. Positive values indicate reductions due to the controls. Attributed to decreased aerosol and gaseous precursor emissions, $PM_{2.5}$ concentrations are generally reduced across the country as a result of the controls, particularly in the north-central, eastern, and south-central regions, currently the most polluted areas in China. The provincial averages of $PM_{2.5}$ concentrations are reduced by 16–27%, 18–24%, and 15–22% for those regions, respectively. Similarly, the depositions of sulfur and base cations are reduced respectively by around 20% and over 50% in those areas. Despite important reductions of NO_X emissions, however, nitrogen deposition is reduced much less than that of sulfur and base cations, since the emissions of NH_3, which contributes significantly to total nitrogen deposition, are taken as unchanged in the two scenarios. Reductions of only 5–7% for nitrogen deposition are found in the north-central, eastern, and south-central areas. As for O_3, concentrations are found to decrease by less than 2.0 $\mu g/m^3$ in most parts of the country, implying that the effects of emission control policies on O_3 are limited. Moreover, higher O_3 concentrations from the controls are found in parts of north-central regions including Beijing, and parts of eastern regions including the Yangtze River Delta and Shanghai. This result suggests that O_3 formation in those areas is dominated by volatile organic compounds (VOC) instead of by NO_X (i.e., it is VOC-limited), as also indicated in other studies (X. Tang et al., 2010; Zhou et al., 2010).

3.2. Health benefits

The health benefits of emission control policies, expressed as the avoided premature deaths in China, are calculated by combining the spatial distributions of concentrations and population across the country. Compared with the base scenario, improvement of air quality under the control scenario implies a mean estimate for avoided death of 55,224, 356,281, and 637 from acute effects of $PM_{2.5}$ exposure, chronic effects of $PM_{2.5}$ exposure, and acute effects of O_3 exposure, respectively. The largest estimated health benefit is from avoided deaths due to reduced chronic exposure of $PM_{2.5}$, equal to approximately 4.0% of all-cause deaths in the country. For O_3, although reduced by the controls in 92% of the simulated area (Fig. 2(b)), the health benefit is comparatively small. This is because: (1) most areas of increased O_3, notably north-central and eastern China, have high population densities; and (2) the effects of O_3 on premature mortality, indicated by the C–R function, are modest compared to those due to $PM_{2.5}$.

Regarding the uncertainties, the 95% CIs of avoided deaths are 9386–82,067, 106,733–627,714, and 289–1046 for acute and chronic effects of $PM_{2.5}$ and acute effects of O_3 respectively, i.e., −47%–49%, −70%–76%, and −55%–64% around the central estimates. The 95% CI of the percentage for avoided all-cause mortality (sum of chronic effects of $PM_{2.5}$ and acute effects of O_3, since the acute effects of $PM_{2.5}$ are considered to be included in the chronic effects) is 1.0%–6.9%. Such large uncertainties result mainly from the uncertainties of the C–R functions. With a large number of grid cells in the modeling domain, the uncertainties of gridded concentrations are reduced through compensations between cells. Since no cohort mortality study is available for China, particular caution is warranted interpreting the chronic health effects of $PM_{2.5}$, which is based on a C–R function derived from a different country and population.

While this study uses the analysis of Pope et al. (2002) for the chronic mortality $PM_{2.5}$ C–R function, Zhou et al. (2010) applied a higher C–R function with larger CI (10% with 95% CI: 1–20%), also obtained from U.S. cohort studies, to the Yangzi River Delta of China. Applying the Zhou et al. (2010) C–R function in this study, the avoided deaths from chronic PM exposure would be reevaluated as 890,702 (95% CI: 137, 988–1,830,569), equal to 9.4% (95% CI: 1.5%–19.8%) of all-cause deaths in the country, as contrasted with the original result of 4.0%. The shapes of C–R functions were suggested as nearly linear, with a leveling off at much higher levels of air pollution (e.g., higher than 15 $\mu g/m^3$ for $PM_{2.5}$) based on the epidemiology studies for the U.S (Pope et al., 2002; Daniels et al., 2000). Given that $PM_{2.5}$ levels in U.S. are generally lower than those in China, the more conservative C–R function by Pope et al. (2002) is tentatively preferred in this study.

Shown in Fig. 3 is the spatial distribution of the avoided premature deaths, combining the effects of reduced chronic $PM_{2.5}$ and O_3 exposure. Significant health benefits are found in the areas with large $PM_{2.5}$ reduction and population densities. The avoided deaths in eastern, south-central and north-central China account for over 80% of the total avoided deaths. This result indicated a significant success for the proposed air pollution control policy judged by the resulting reduction of public health damage, particularly in areas currently suffering the heaviest air pollution.

3.3. Effects on soil acidification

Through a comparison of the simulated depositions of sulfur, nitrogen and base cations on the basis of CL, the distributions of CL exceedances in the base and control scenarios in 2020 are estimated and shown in Fig. 4. In the base case, the areas exceeding CL will cover approximately 18% of China's mainland territory, especially in south-central, southwestern, and parts of eastern and northeastern China. The total exceedance for the country is estimated at 2.8 Mt sulfur, equaling 18% of national SO_2 emissions in the scenario. In the control scenario, even with significant reductions in sulfur depositions, the area exceeding CL will remain 18% and the total exceedance will decrease slightly to 2.4 Mt of sulfur, indicating minimal benefits from acidification control. This is due mainly to the PM emission controls with consequent reduced alkaline dust available to counteract acidification. Moreover, the CL exceedances of both scenarios in 2020 are greater than those in 2005, in which the area exceeding CL

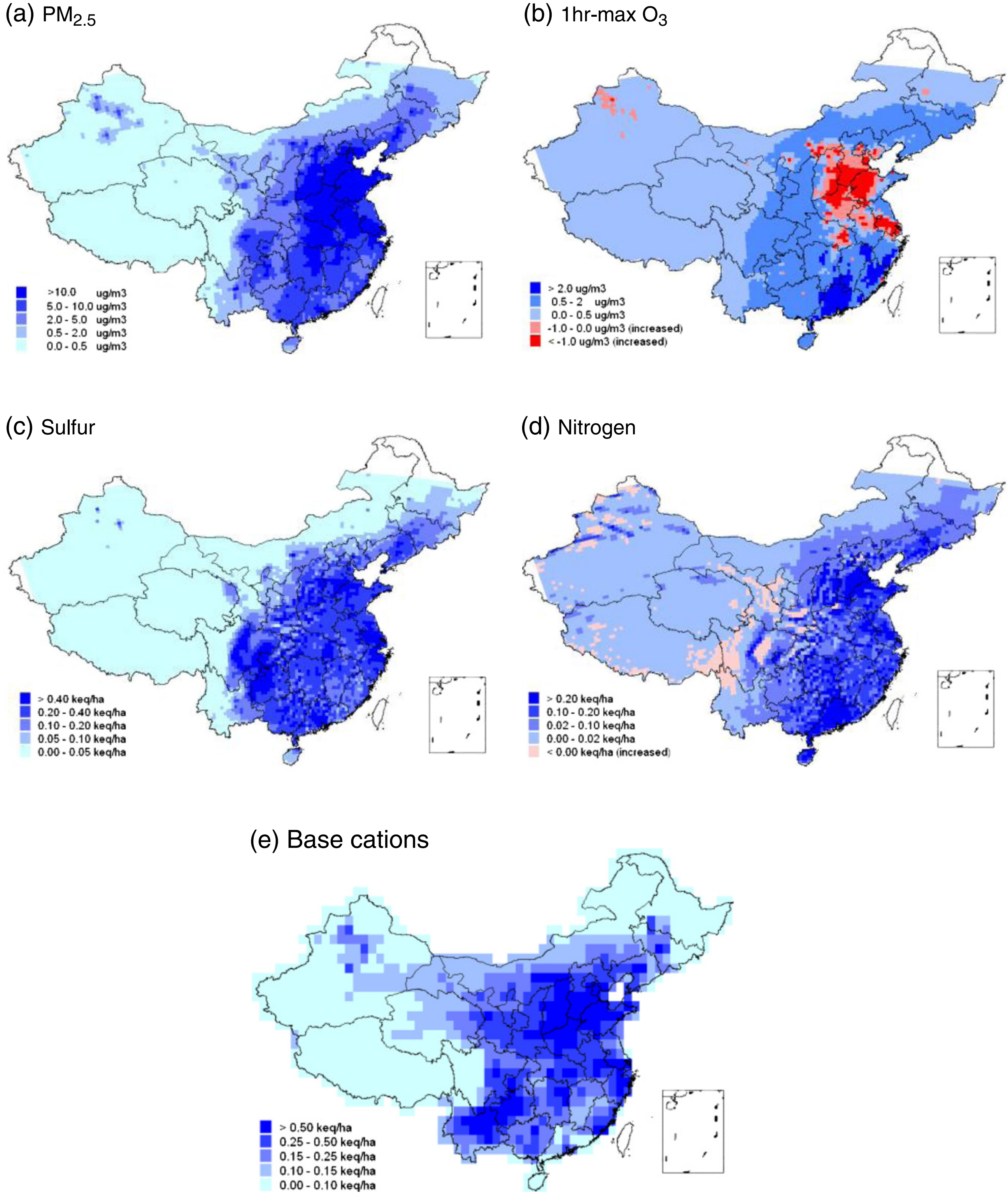

Fig. 2. Difference of simulated annual concentrations and depositions between the base and control scenarios in 2020 (Control–base). (a) $PM_{2.5}$ (b) 1 h-max O_3; (c) Sulfur; (d) Nitrogen; (e) Base cations. Due to a limitation of the modeling domain, there are no results for small regions in the far northeast and northwest for (a)–(d).

is estimated at 16% with total exceedance of 2.2 Mt sulfur, respectively (Zhao et al., 2011b). This result indicates that anthropogenic PM emission control in China may undermine any benefits to soil acidification expected from SO_2 and NO_X control. This conclusion is supported partly by the limited available field observations. Long-term monitoring indicates that increasing acidities at many sites across China may be attributed partly to the decrease in concentrations of airborne PM (J. Tang et al., 2010).

Cumulative distributions of CL exceedances are compared in Fig. 5(a) for the scenarios in 2020 and 2005. Higher curves indicate relatively lower acidification risks at the national level. In 2005, for example, roughly 85% of the country's territory did not exceed the

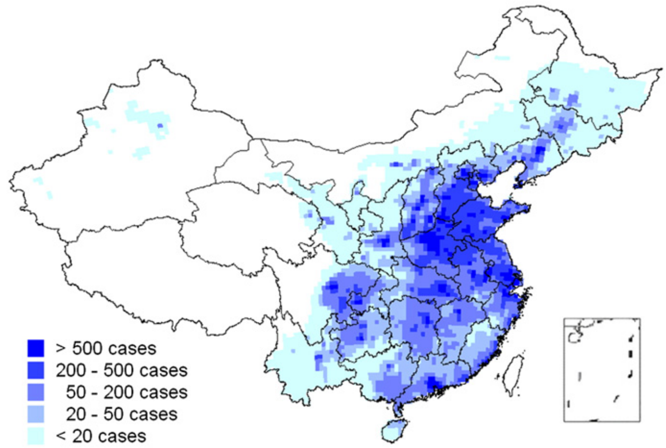

Fig. 3. Health benefits of emission control policies in 2020, expressed as avoided deaths/grid.

critical load; the remaining 15% suffered varied levels of soil acidification, represented by CL exceedances that increase from left to right until 100% of the territory is accounted for. It is clear that soil acidification at the national level will increase from 2005 to 2020 absent more stringent emission control policies (from the solid black curve to the thin black one). Slight improvements will be achieved under the policies assumed in the 2020 control scenario (from the thin black to the thin gray), although the benefits of reducing acidic gaseous pollutants may be counteracted by concomitant reductions in emissions of alkaline dust.

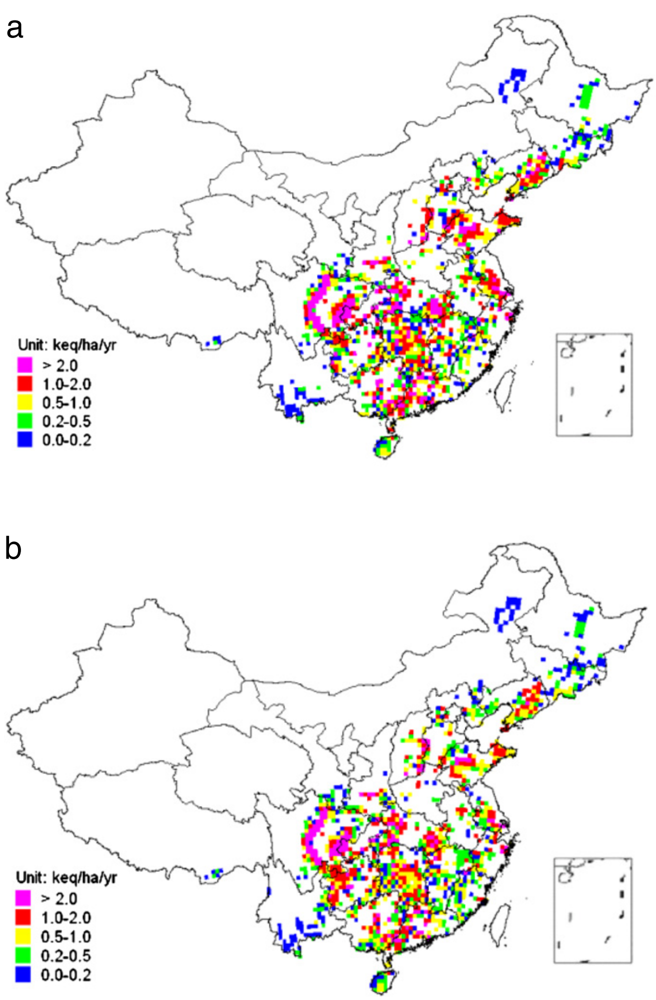

Fig. 4. The critical load exceedance in 2020. (a) Base scenario; (b) Control scenario.

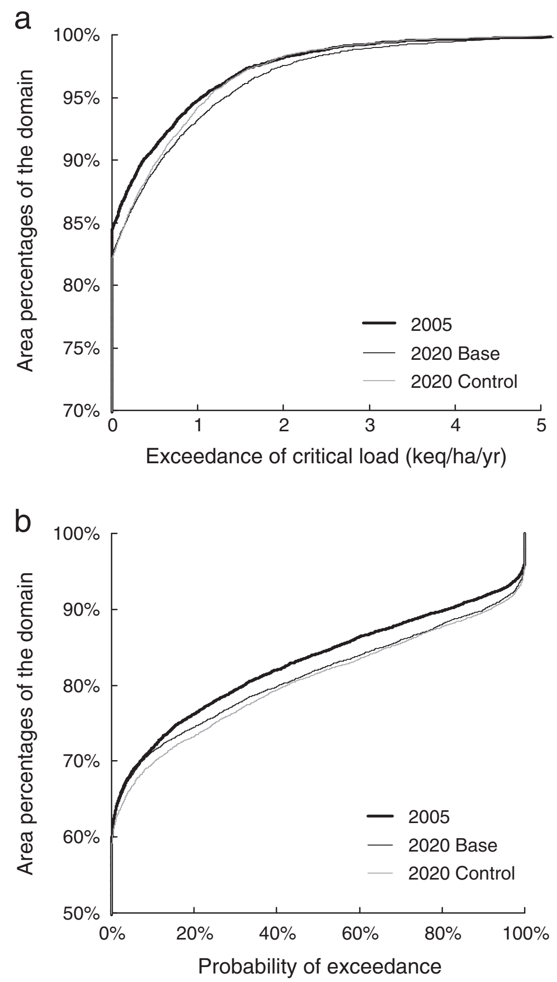

Fig. 5. The cumulative distributions of areas of (a) exceedance of critical loads, and (b) probability of exceedance. Higher curves indicate relatively lower acidification risks at the national level. In panel (a), for example, roughly 85% of the country's territory did not exceed the critical load in 2005; the remaining 15% suffers varied levels of soil acidification, represented by CL exceedances that increase from left to right until 100% of the territory is accounted for.

When the uncertainty in CL calculation is factored in, however, the results differ. Shown in Fig. 5(b) are the cumulative distributions of CL exceedance probability for 2005 and the two scenarios in 2020. For all cases, approximately 60% of the country's territory is estimated to be 100% safe from soil acidification; the remaining 40% has varied probabilities of CL exceedance from 0 to 100%. For example, the area percentages with a probability of CL exceedance larger than 20% are 23.8%, 25.5%, and 26.7% for 2005, base 2020, and control 2020 scenarios, respectively; those values change to 15.8%, 18.0%, and 18.4%, respectively, for a probability of 50%. These numbers imply a slightly higher acidification risk for the control scenario than the base scenario in 2020, which is inconsistent with Fig. 5(a). The difference results from the large uncertainties of CL as shown in Fig. 6, with an average 95% CI of −64%–112% around the central estimate for all the grid cells in the domain. Among all relevant parameters, the uncertainties of BCs_W are estimated to contribute most to the variance of CLs over 82% of the national territory, followed by BCs_D with 12%. The accuracy

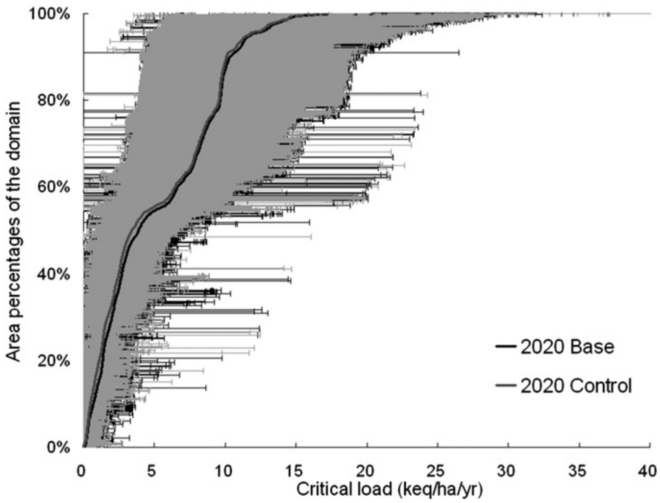

Fig. 6. The cumulative distributions of areas of critical loads for the base (black) and control (gray) scenarios. The horizontal bars represent 95% CIs of critical loads.

of weathering rates of base cations in the soil minerals, and that of atmospheric depositions of base cations, are crucial in the CL calculations and thus in analyses of soil acidification in China.

3.4. Effects on global temperature

The global temperature changes due to variations of Chinese emissions from 2005 to 2020 are estimated as −0.011 K and 0.064 K for the base and control scenarios, respectively, as shown in Fig. 7(a). The cooling in the base scenario results mainly from increased emissions of NO_X and thus higher concentrations of nitrate aerosols. Slight changes of other species including SO_2, BC, and OC are estimated to have modest warming effects. With tightened control measures, however, much larger warming effect results from the sizable reduction of SO_2 emissions. The cooling effect from reduced BC only slightly compensate for the warming effect from decreased SO_2 emissions. This result indicates that the anticipated emission control policies in the near future would not reduce climate warming, and that policies specifically targeting BC and greenhouse gases (GHGs) will be required.

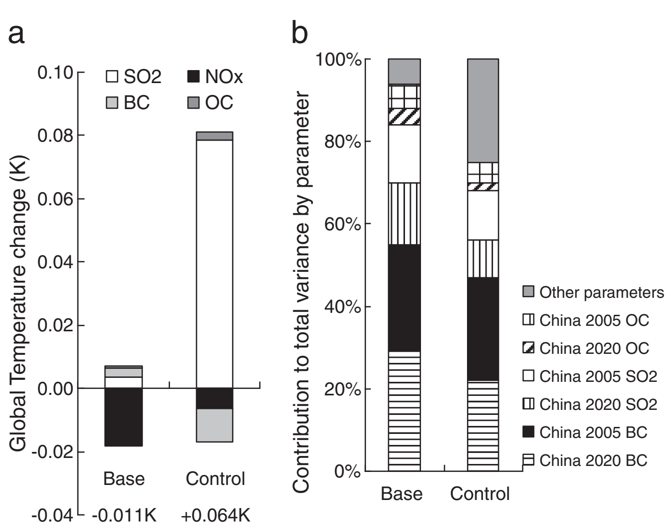

Fig. 7. (a) Effects of changes of Chinese emissions from 2005 to 2020 on global temperature; (b) the contributions of different parameters to the variance of the global temperature response.

The 95% CIs of the temperature changes are estimated as −0.182–0.126 K and −0.077–0.269 K for the base and control scenarios, respectively, implying extremely large uncertainties. Shown in Fig. 7 (b) are the contributions of different parameters to the variances of the estimated temperature changes. The contributions to the variances by Chinese BC emissions are respectively estimated as 55% and 47% for the base and control scenarios, followed by those by SO_2 and OC. The emission uncertainties of these three species are responsible for 94% and 75% of the variance in the base and control scenarios, respectively. The uncertainties in the remaining parameters, including climate sensitivity, constituent global forcing, and global emissions are less important, with the exception of CGF_{SO2} which accounts for 16% of the variance in the control scenario. Although the uncertainty of Chinese BC emissions is significantly reduced compared to prior estimates (Zhao et al., 2011a), it remains the dominant factor for the uncertainties of global temperature change in this study. To better understand the relationship of global climate change and Chinese emissions, further field measurements are recommended on emission factors for BC in industrial and residential boilers burning solid fuels such as coal briquettes and biomass. These are recognized as main contributors to uncertainties in BC emissions for China (Aunan et al., 2009; Zhao et al., 2011a).

In this study, the global average CGF is applied to estimate the effects on temperature changes due to variations of Chinese emissions. However, it should be noted that the radiative forcing and the forcing efficacy from short-lived species were found to be different across the globe, due to heterogeneous chemical, physical and meteorological environments. Specifically, the energy changes of the earth-atmospheric system per unit mass of sulfur, BC and OC emissions from East Asia are reported to be smaller than those from most of other regions in the world (Berntsen et al., 2006; Bond et al., 2011). A more serious warming effect may thus appear if an equal emission reduction for short-lived species included in this study is achieved in those regions other than China, since the temperature increase from emission control is dominated by the decline of SO_2 emissions. Nevertheless, we mean that the effect of geographic difference on radiative forcing and temperature response is modest in this study, because (1) the relative variations of radiative forcing due to geographic difference are smaller than those of CGF we assumed in the uncertainty analysis; and (2) the uncertainties of CGF contributed smaller to the total variance of temperature responses than those of China's BC emissions did.

4. Conclusions

Multiple effects of air pollution control policies from 2005 to 2020 in China are estimated and presented with uncertainties, using a scenario analysis method. In general, the effects of current air pollution control in China are estimated to be in conflict, and more effort should be made to reconcile different environmental objectives. The main findings are as follows:

(1) A mean estimate of 4% for all-cause mortality in the country in 2020 can be avoided by anticipated air pollution controls, particularly in the regions with highest population densities and the most serious air pollution. The major benefits to public health result from reductions in aerosols but not from O_3, which is expected to increase in parts of north-central and eastern China as a result of NO_X control measures.

(2) Recovery from soil acidification may be delayed or even reversed despite decreasing SO_2 emissions. This is attributed to the fact that depositions of base cations, the main species counteracting acidification, are expected to decline concurrently with acid precursors, through PM emission control measures implemented in cement and other industrial production. More stringent policies to control SO_2, NO_X, and NH_3 should thus be considered to prevent further soil acidification.

(3) Current air pollution control measures are unlikely to reduce risks of climate warming, since significant reductions in SO_2 emissions will reduce the cooling impact of reflective aerosols. This result, however, is uncertain, reflecting the major uncertainty in estimates for BC emissions in China.

Emissions of a number of other species that also play important roles in different environmental concerns are not included in this study, since explicit national control policies are lacking. For example, changes CH_4 emissions, a primary GHG, are expected to influence tropospheric O_3 levels and thereby air quality and public health (West and Fiore, 2005). Changes in emissions of non-methane volatile organic compounds (NMVOC) are expected to impact the lifetime of CH_4 and thus climate, and to change tropospheric O_3 levels, particularly in the VOC-limited regions like north-central and parts of eastern China. Emissions of CO_2, of which the major sources are also sources of air pollutants, will be influenced by national energy policies and emission control measures. Given such comprehensive effects, trends in emission of GHG species should be integrated with those of criteria pollutants in a multiple-effects framework. Better targeted emission control measures are needed to efficiently mitigate local and regional air pollution and global warming.

Acknowledgment

This work was sponsored by the U.S. National Science Foundation (Grant ATM-1019134).

References

Aunan K, Pan XC. Exposure–response functions for health effects of ambient air pollution applicable for China—a meta analysis. Sci Total Environ 2004;329:3-16.

Aunan K, Berntsen TK, Myhre G, Rypdal K, Streets DG, Woo J-H, et al. Radiative forcing from household fuel burning in Asia. Atmos Environ 2009;43:5674–81.

Berntsen T, Fuglestvedt J, Myhre G, Stordal F, Berglen TF. Abatement of greenhouse gases: does location matter? Climatic Change 2006;74:377–411.

Bond TC, Streets DG, Yarber KF, Nelson SM, Woo J-H, Klimont Z. A technology-based global inventory of black and organic carbon emissions from combustion. J Geophys Res 2004;109. Art. No. D14203.

Bond TC, Zarzycki C, Flanner MG, Koch DM. Quantifying immediate radiative forcing by black carbon and organic matter with the specific forcing pulse. Atmos Chem Phys 2011;11:1505–25.

Carmichael GR, Streets DG, Calori G, Amann M, Jacobson MZ, Hansen J, et al. Changing trends in sulfur emissions in Asia: implications for acid deposition, air pollution, and climate. Environ Sci Technol 2002;36:4707–13.

Centre on Emission Inventories and Projections (CEIP). Officially reported emission data. available at:http://www.ceip.at2010.

China Data Center (CDC). China 2000 County Population Census. University of Michigan; 2003.

Chinese Academy for Environmental Planning (CAEP), State Information Center (SIC). Environmental and economical forecasting report. Beijing: Chinese Environmental Science Press; 2009 (in Chinese).

Cofala J, Amann M, Klimont Z, Kupiainen K, Hoglund-Isaksson L. Scenarios of global anthropogenic emissions of air pollutants and methane until 2030. Atmos Environ 2007;41:8486–99.

Daniels MJ, Dominici F, Samet JM, Zeger SL. Estimating particulate matter-mortality dose–response curves and threshold levels: an analysis of daily time-series for the 20 largest US cities. Am J Epidemiol 2000;152:397–406.

Dockery DW, Pope CA. Acute respiratory effects of particulate air pollution. Annu Rev Publ Heath 1994;15:107–32.

Duan L, Hao JM, Xie SD, Zhou ZP, Ye XM. Determining weathering rates of soils in China. Geoderma 2002;110:205–25.

Duan L, Huang YM, Hao JM, Xie SD, Hou M. Vegetation uptake of nitrogen and base cations in China and its role in soil acidification. Sci Total Environ 2004;330:187–98.

Duan L, Lin Y, Zhu XY, Tang GG, Gao DF, Hao JM. Modeling atmospheric transport and deposition of calcium in China. J Tsinghua Univ (Sci Technol) 2007;47:1462–5. (in Chinese).

Fu JS, Streets DG, Jang CJ, Hao JM, He KB, Wang LT, et al. Modeling regional/urban ozone and particulate matter in Beijing, China. J Air Waste Manage Assoc 2009;59:37–44.

Hao JM, Wang SX, Liu BJ, He KB. Designation of acid rain and SO_2 pollution control zones and control policies in China. J Environ Sci Health Part A 2000;35:1901–14.

Hao JM, Duan L, Zhou XL, Fu LX. Application of a LRT model to acid rain control in China. Environ Sci Technol 2001;35:3407–15.

Health Effects Institution (HEI). Special report 15 health effects of outdoor air pollution in developing countries of Asia: a literature review; 2004.

Hettelingh J-P, Posch M, Slootweg J, Reinds GJ, Spranger T, Tarrason L. Critical loads and dynamic modelling to assess European areas at risk of acidification and eutrophication. Water Air Soil Pollut 2007:379–84. Focus 7.

Hettelingh J-P, Posch M, Slootweg J, editors. Critical load, dynamic modelling and impact assessment in Europe, CCE Status Report; 2008.Report No. 500090003, Available athttp://www.pbl.nl/en/publications/2009/Critical-load-dynamic-modelling-and-impact-assessment-in-Europe-CCE-Status-Report-2008.html.

Heywood L, Hall J, Smith R. Uncertainty in mass balance critical loads and exceedance: application to a UK national data set. Atmos Environ 2006;40:6146–53.

Ho MS, Nielsen CP, editors. Clearing the air: the health and economic damages of air pollution in China. Cambridge, MA: MIT Press; 2007.

Intergovernmental Panel on Climate Change (IPCC). Climate Change 2007 — the physical science basis. Contribution of Working Group I to the Fourth Assessment Report of the IPCC; 2007.

International Energy Agency (IEA). World energy outlook 2007: China and India insights; 2007.

Klimont Z, Cofala J, Xing J, Wei W, Zhang CY, Wang SX, et al. Projections of SO_2, NO_X, and carbonaceous aerosols emissions in Asia. Tellus Ser B 2009;61B:602–17.

Larssen T, Carmichael GR. Acid rain and acidification in China: the importance of base cation deposition. Environ Pollut 2000;110:89-102.

Larssen T, Lydersen E, Tang DG, He Y, Gao JX, Liu HY, et al. Acid rain in China. Environ Sci Technol 2006;40:418–25.

Lei Y, Zhang Q, Nielsen CP, He KB. An inventory of primary air pollutants and CO_2 emissions from cement industry in China, 1990–2020. Atmos Environ 2011;45:147–54.

Levy JI, Carrothers TJ, Tuomisto JT, Hammitt JK, Evans JS. Assessing the public health benefits of reduced ozone concentrations. Environ Health Perspect 2001;109:9-20.

Li H, McNulty SG. Uncertainty analysis on simple mass balance model to calculate critical loads for soil acidity. Environ Pollut 2007;149:315–26.

Lin JT, Nielsen CP, Zhao Y, Lei Y, Liu Y, McElroy MB. Recent changes in particulate air pollution over China observed from space and the ground: effectiveness of emission control. Environ Sci Technol 2010;44:7771–6.

Lou SJ, Zhu B, Liao H. Impacts of O_3 precursor on surface O_3 concentration over China. Trans Atmos Sci 2010;33:451–9. (in Chinese).

Ministry of Environmental Protection (MEP). Chinese Environment Communique 2008. available at:http://www.mep.gov.cn2009.

National Bureau of Statistics of China (NBS). Chinese statistical yearbook. Beijing: China Statistics Press; 2006 (in Chinese).

National Population Development Strategy Research (NPDSR). Research report on national population development strategy. available at:http://www.gov.cn/2007. (in Chinese).

Ohara T, Akimoto H, Kurokawa K, Horii N, Yamaji K, Yan X, et al. An Asian emission inventory of anthropogenic emission sources for the period 1980–2020. Atmos Chem Phys 2007;7:4419–44.

Pope CA, Burnett RT, Thun MJ, Calle EE, Krewski D, Ito K, et al. Lung cancer, cardiopulmonary mortality, and long-term exposure to fine particulate air pollution. J Am Med Assoc 2002;287:1132–41.

Saikawa E, Naik V, Horowitz LW, Liu JF, Mauzerall DL. Present and potential future contributions of sulfate, black and organic carbon aerosols from China to global air quality, premature mortality and radiative forcing. Atmos Environ 2009;43:2814–22.

Skeffington RA, Whitehead PG, Abbott J. Quantifying uncertainty in critical loads: (B) acidity mass balance critical loads on a sensitive site. Water Air Soil Pollut 2006;169:25–46.

Skeffington RA, Whitehead PG, Heywood E, Hall JR, Wadsworth RA, Reynolds B. Estimating uncertainty in terrestrial critical loads and their exceedances at four sites in the UK. Sci Total Environ 2007;382:199–213.

Streets DG, Bond TC, Carmichael GR, Fernandes SD, Fu Q, He D, et al. An inventory of gaseous and primary aerosol emissions in Asia in the year 2000. J Geophys Res 2003;108(D21). Art. No. 8809.

Streets DG, Fu JHS, Jang CJ, Hao JM, He KB, Tang XY, et al. Air quality during the 2008 Beijing Olympic Games. Atmos Environ 2007;41:480–92.

Tang J, Xu XB, Ba J, Wang SF. Trends of the precipitation acidity over China during 1992–2006. Chin Sci Bull 2010a;55:1800–7.

Tang X, Wang ZF, Zhu J, Gbaguidi AE, Wu QZ, Li J, et al. Sensitivity of ozone to precursor emissions in urban Beijing with a Monte Carlo scheme. Atmos Environ 2010b;44:3833–42.

U.S. Environmental Protection Agency (USEPA). National emission inventory (NEI) air pollutant emissions trends data. available at:http://www.epa.gov/ttn/chief/trends/index.html2010.

UBA. Manual on methodologies and criteria for modelling and mapping critical loads and levels and air pollution effects, risks and trends. Berlin: Umweltbundesamt; 2004.

Wang WX, Xu PJ. Research progress in precipitation chemistry in China. Prog Chem 2009;21:266–81.

Wang M, Huo H, Johnson L. Projection of Chinese motor vehicle growth, oil demand, and CO_2 emissions through 2050. Argonne National Laboratory; 2006a. ANL/ESD/06-6.

Wang T, Ding A, Gao J, Wu WS. Strong ozone production in urban plumes from Beijing, China. Geophys Res Lett 2006b;33. Art. No. L21806.

Wang LT, Hao JM, He KB, Wang SX, Li JH, Zhang Q, et al. A modeling study of coarse particulate matter pollution in Beijing: regional source contributions and control implications for the 2008 Summer Olympics. J Air Waste Manage Assoc 2008;58:1057–69.

West JJ, Fiore AM. Management of tropospheric ozone by reducing methane emissions. Environ Sci Technol 2005;39:4685–91.

Wong CM, Vichit-Vadakan N, Kan HD, Qian ZM, the PAPA Project Teams. Public health and air pollution in Asia (PAPA): a multicity study of short-term effects of air pollution on mortality. Environ Health Perspect 2008;116:1195–202.

World Bank (WB), State Environmental Protection Administration (SEPA). Cost of pollution in China. available at:http://www.worldbank.org/eapenvironment2007.
Xing J, Wang SX, Chatani S, Cofala J, Klimont Z, Amann M, et al. Validation of an integrated gridded emission inventory for China by satellite and surface observation. Submitted to Atmos Environ.
Zhang Y, Liu P, Pun B, Seigneur C. A comprehensive performance evaluation of MM5-CMAQ for the Summer 1999 Southern Oxidants Study episode, Part I. Evaluation protocols, databases and meteorological predictions. Atmos Environ 2006;40:4825–38.
Zhang Q, Streets DG, He KB, Wang YX, Richter A, Burrows JP, et al. NO_X emission trends for China, 1995–2004: the view from the ground and the view from space. J Geophys Res 2007;112(D22). Art. No. D22306.
Zhang Y, Vijayaraghavan K, Wen XY, Snell HE, Jacobson MZ. Probing into regional ozone and particulate matter pollution in the United States: 1. A 1 year CMAQ simulation and evaluation using surface and satellite data. J Geophys Res 2009;114. Art. No. D22304.
Zhao Y, Duan L, Larssen T, Hu LH, Hao JM. Simultaneous assessment of deposition effects of base cations, sulfur, and nitrogen using an extended critical load function for acidification. Environ Sci Technol 2007;41:1815–20.
Zhao Y, Wang SX, Duan L, Lei Y, Cao PF, Hao JM. Primary air pollutant emissions of coal-fired power plants in China: current status and future prediction. Atmos Environ 2008;42:8442–52.
Zhao Y, Duan L, Xing J, Larssen T, Nielsen CP, Hao JM. Soil acidification in China: is controlling SO_2 emissions enough. Environ Sci Technol 2009;43:8021–6.
Zhao Y, Wang SX, Nielsen CP, Li XH, Hao JM. Establishment of a database of emission factors for atmospheric pollutants from Chinese coal-fired power plants. Atmos Environ 2010;44:1515–23.
Zhao Y, Nielsen CP, Lei Y, McElroy MB, Hao JM. Quantifying the uncertainties of a bottom–up emission inventory of anthropogenic atmospheric pollutants in China. Atmos Chem Phys 2011a;11:2295–308.
Zhao Y, Duan L, Lei Y, Xing J, Nielsen CP, Hao JM. Will PM control undermine China's efforts to reduce soil acidification? Environ Pollut 2011b;159:2726–32.
Zhou Y, Fu JS, Zhuang GS, Levy JI. Risk-based prioritization among air pollution control strategies in the Yangzi River Delta, China. Environ Health Perspect 2010;118:1204–10.